Defence Research and Development Canada
Recherche et développement pour la défense Canada

DRDC | RDDC
technologysciencetechnologie

Modeling and Experimental Support for Detection of Linear Conductors
Task Authorization 4: Ground Properties Sensor

Prepared by:
C-CORE Project Team: Dave Green (Project Manager), Chris Fowler, Mike Royle
Captain Robert A. Bartlett Building
Morrissey Road
St. John's, NL Canada A1B 3X5
C-CORE Report Number R-17-038-1336, Revision 1.1

PSPC Contract Number: W7702-175832
Technical Authority: Scott Irvine, Defence Scientist
Contractor's date of publication: March 2018

Defence Research and Development Canada
Contract Report
DRDC-RDDC-2019-C019
January 2019

Canada

IMPORTANT INFORMATIVE STATEMENTS

This document was reviewed for Controlled Goods by Defence Research and Development Canada using the Schedule to the *Defence Production Act*.

Modeling and Experimental Support for Detection of Linear Conductors

Task Authorization 4: Ground Properties Sensor

C-CORE Report Number
R-17-038-1336

Prepared for:
DRDC Suffield

Revision 1.1
March, 2018

Captain Robert A. Bartlett Building
Morrissey Road
St. John's, NL
Canada A1B 3X5

T: (709) 864-8354
F: (709) 864-4706

Info@c-core.ca
www.c-core.ca

Registered to ISO 9001:2008

This page is intentionally left blank

Modeling and Experimental Support for Detection of Linear Conductors

Task Authorization 4: Ground Properties Sensor

Prepared for:
DRDC Suffield

Prepared by:
C-CORE

C-CORE Report Number:
R-17-038-1336
Revision 1.1
March, 2018

Captain Robert A. Bartlett Building
Morrissey Road
St. John's, NL
Canada A1B 3X5

T: (709) 864-8354
F: (709) 864-4706
Info@c-core.ca
www.c-core.ca

Registered to ISO 9001:2008

The correct citation for this report is:
C-CORE. 2018. "Modeling and Experimental Support for Detection of Linear Conductors—Task Authorization 4: Ground Properties Sensor." Report R-17-038-1336, Revision 1.1.

Project Team

Dave Green (Project Manager)
Chris Fowler
Mike Royle

REVISION HISTORY

VERSION	NAME	DATE OF CHANGES	COMMENTS
1.0	D. Green	11/30/2017	Released to client
1.1	D. Green	03/07/2018	Released to client
1.2	D. Green	25/06/2018	Released to client

DISTRIBUTION LIST

COMPANY	NAME	NUMBER OF COPIES
DRDC Suffield	Dr. Scott Irvine	Electronic

Table of Contents

List of Tables

List of Figures

1 Introduction

There is an ongoing research program at Defence Research and Development Canada (DRDC) Suffield Research Centre (SRC) to explore electromagnetic (EM) scattering from linear conductors to better understand the physical phenomena governing this effect. The purpose of this contract is to provide technical expertise to supplement the efforts at DRDC by furthering the research on EM scattering through experimental and theoretical means.

The need to detect linear conductors is pertinent to military and commercial interests. A number of commercial applications would benefit from a reliable method to detect buried infrastructure such as wires, pipes, rods and other infrastructure critical to the delivery of crucial services to consumers. Detection of these conductors would help to significantly reduce the number of occurrences resulting in interruptions to power, water and communications services that result from excavation operations. This would directly result in time and money savings for businesses and consumers alike and help alleviate associated safety and environmental concerns.

A principal factor in buried conductor detection is consideration of the ground properties. In particular, the conductivity and relativity permittivity of the soil can have impacts on the propagation of transmitted waves and reradiated fields (C-CORE 2013), as well as the resonances that can be developed in a length of conductor (C-CORE 2014) for schemes which exploit this.

This work has been carried out under Task Authorization (TA) 4 entitled “Ground Properties Sensor.” This TA is authorized under contract No. W7702-175832/001/EDM with DRDC Suffield.

1.1 Scope

This report provides an overview of the work carried out to develop and test a sensor capable of measuring ground properties, in particular the conductivity and permittivity. The sensor design is described in detail. Test results from a functional test are also presented demonstrating the proof of concept. Future improvements are also recommended such that a more field-ready prototype could be designed and implemented.

1.2 Definitions

Acronym	Definition
ADC	Analog Digital Converter
COTS	Commercial Off-The-Shelf
DDS	Direct Digital Synthesizer
DRDC	Defence Research and Development Canada
EM	Electromagnetic
GUI	Graphical User Interface
ITU	International Telecommunications Union
PC	Personal Computer
PCB	Printed Circuit Board

Acronym	Definition
RF	Radio Frequency
SRC	Suffield Research Centre
TA	Task Authorization
TRL	Technological Readiness Level
USB	Universal Serial Bus

2 Background

An ongoing program at DRDC SRC involves the detection of linear conductors on the surface or below the ground using electromagnetic sensing methods. The properties of the ground have a large impact on the viability of such detection schemes. A couple of examples where the importance of ground properties has arisen in prior contracts are listed below:

- For a proposed detection scheme involving exploiting transmitters of opportunity (C-CORE 2013), the ground properties dictate the propagation of the transmitted ground wave. That is, a more conductive ground (i.e., wetter ground) allows better ground wave transmission and a higher received field at a given range (International Telecommunications Union 2007).
- A more conductive ground is less conducive to penetration of primary radiated fields for applications of buried conductors (C-CORE 2013, 2014). Hence it will limit the degree to which the primary field will induce currents in the conductor, as well as the strength of the secondary field received back above the surface.
- Ground properties also have a significant effect on the effective conductor length when determining the resonant frequencies for methods which exploit this phenomenon (C-CORE 2014).

There is therefore great value in *a priori* knowledge of the surrounding ground properties when designing or implementing a detection scheme. The ground properties can be fed into models which predict the behaviour of conductors in the presence of radiated fields, and thereby streamline the synthesis of a detection scheme. The properties could also be used as inputs for a detection system to optimize its performance in a particular locale.

3 Prototype Design

The design of the proof-of-concept prototype is largely based on that proposed in a prior report (C-CORE 2017). This design comprises two major sections: a transmitter which injects a steady radio frequency (RF) current into the ground with two probes, and a receiver which receives a resulting field across two probes. The schematics for this design are in drawing DEA-1336-1000 found in Appendix A.

3.1 Transmitter

The transmitter uses a direct digital synthesizer (DDS) module (U3) controlled by a microcontroller to generate a transmission frequency. The relevant portion of the schematic is shown in Figure 1. The prototype is set up to generate a lower frequency (100 kHz) and a higher frequency (1 MHz). The microcontroller directs the DDS to switch between these two frequencies at roughly one second intervals. That is, one second of 100 kHz, followed by one second of 1 MHz, and then repeated indefinitely. This is because it was noted in a prior report that conductivity is more easily measured at lower frequencies, and permittivity at higher frequencies. Note that the DDS is provided in an evaluation board, which has all the necessary support components and interfacing circuitry. For a future iteration of this prototype, a custom printed circuit board (PCB) could be created that incorporates the necessary elements of the evaluation board.

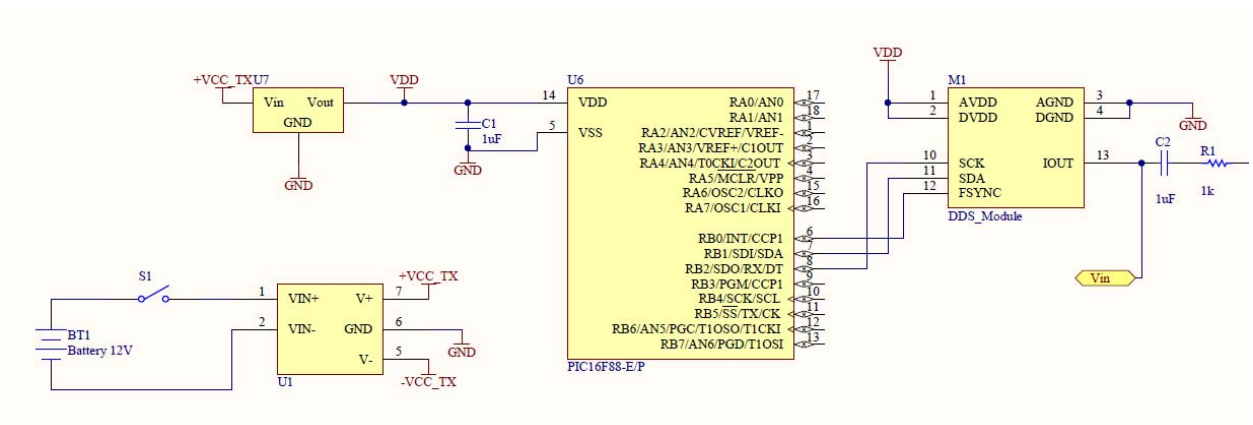

Figure 1. Microcontroller and DDS circuitry.

The output signal of the DDS module is then fed into a series of operational amplifier circuits which behave as a current source amplifier. The relevant portion of the schematic is depicted in Figure 2. U3 and U4 are standard inverting amplifiers—two are required to split the desired gain in order to keep their individual gains well below the 200 MHz gain bandwidth product of the LM7171. U5 is a non-inverting amplifier which senses the current passing through the two probes (P1 and P2). This output is added to the summing node formed by R3 and R5 to give feedback to the amplifier U4. The result is an amplifier which strives to maintain a consistent RF current through the two probes. The series resistance R6 is added to the anticipated ground resistance. This “bias” resistance ensures greater compliance of the current source.

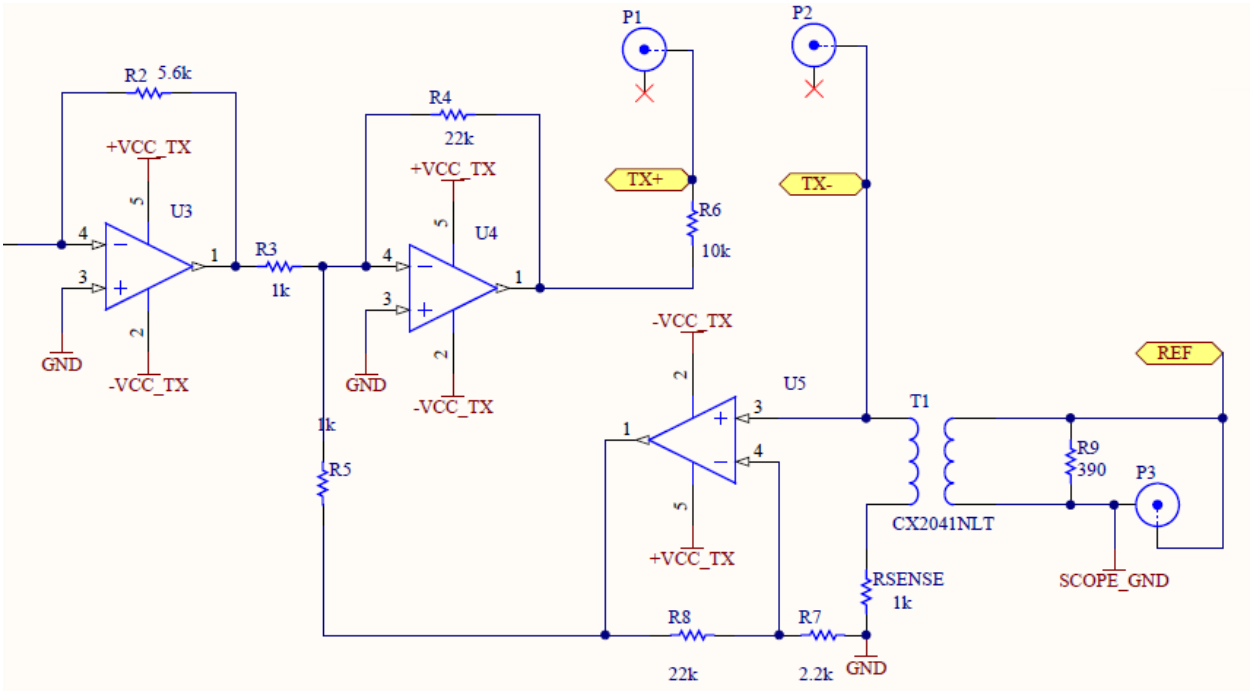

Figure 2. Operational amplifier circuitry.

A signal transformer (T1) with a unity turn ratio is used to magnetically isolate the current signal used in feedback. This is then supplied at P3 to be connected to the data acquisition system (Section 3.3). The intention is to provide a phase reference so that phase information can be used for determining ground permittivity.

3.2 Receiver

The receiver comprises a straightforward differential amplifier circuit (U8) to amplify the received signal across P4 and P5 to levels that can be accepted within the dynamic range of the data acquisition system. The relevant circuitry is found in Figure 3. For this prototype system, a gain of 100 was arbitrarily selected; it can easily be changed by adjusting R13 and R14. The output is presented on P6.

Note that the receiver and the transmitter are powered from different batteries to ensure that there is no direct coupling of the transmitted signal to the receiver. Also, both receiver and transmitter circuitry were enclosed in metal cases to shield the circuitry from external interference.

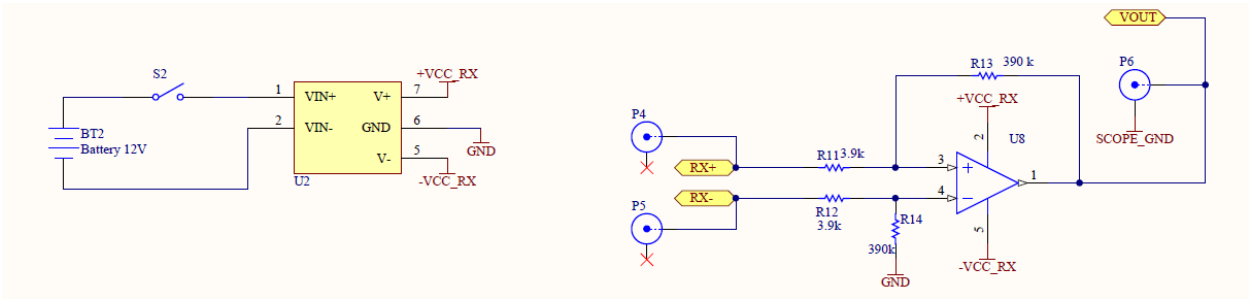

Figure 3. Receiver circuitry.

3.3 Data Acquisition System

For this prototype, a PicoScope 2206B personal computer (PC)-based oscilloscope was used as the data acquisition system. It allows simultaneous capture of two signals: the received signal itself from P6, and the reference signal from P3. It is connected to a laptop PC via Universal Serial Bus (USB), and draws its power from the USB port.

Custom software with a simple graphical user interface (GUI) was written for the PicoScope to facilitate recording measurements. A screenshot is seen in Figure 4. It allows the user to enter the lower and higher frequencies that should be examined. The defaults are 100 kHz and 1 MHz as outlined in Section 3.1, however, it is possible to reprogram the microcontroller if other frequencies are desired. The software captures a stream of 100,000 samples at a rate of 20.833 MS/s for both the received signal channel and the reference signal channel. The discrete Fourier transform is calculated at the two frequencies specified for each channel. The magnitude and phase of the Fourier coefficient is recorded in the specified file, for both frequencies, and for both channels.

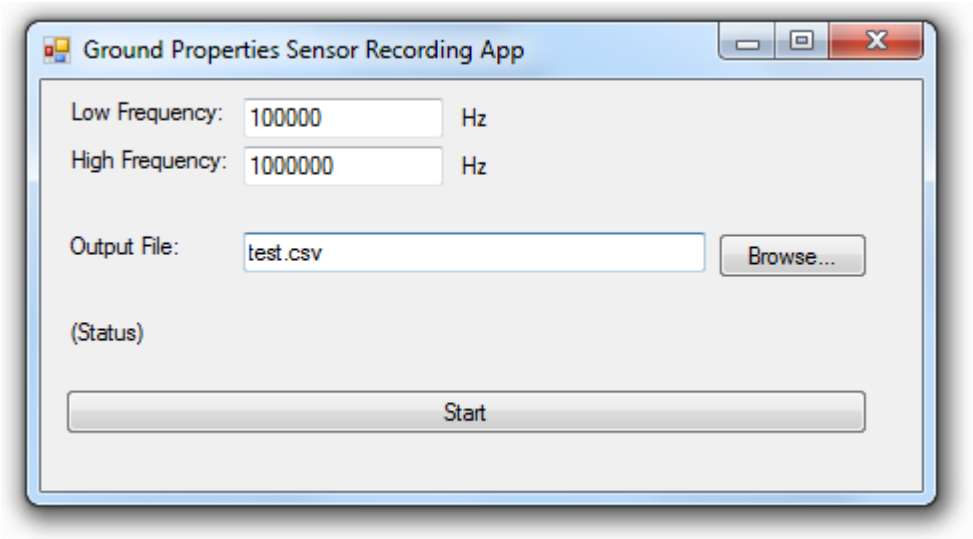

Figure 4. Measurement recording software GUI.

3.4 Frame

Construction of the frame proposed in a prior report was not attempted owing to cost constraints. The frame for this prototype was constructed from 2x4 and 2x2 dimensional lumber. The completed assembly is shown in Figure 5.

Figure 5. Setup of ground properties sensor.

The frame is 1m x 1m as prescribed in the background report (C-CORE 2017). The frame is mounted to a pair of wheels to allow easy movement over the ground. Four “legs” are hinged from each of the corners of the frame, and have a metal caster at the bottom of each. These casters are the probe terminals used for the transmitter and receiver. Each caster is electrically connected to the center conductor of an RF connector. This allows easy attachment of a cable from the caster to the receiver input terminals or transmitter output terminals. By having the legs hinged, it is possible to move the sensor frame and have the casters maintain contact with the ground at all times regardless of minor perturbations in the ground surface.

4 Testing

The functioning of the ground properties sensor was verified by taking readings for the same region of ground but with different properties. The ground properties were artificially altered by pouring 7.5 litres of water on the ground under and immediately surrounding the sensor frame with a watering can. This corresponds to a rainfall event of approximately 7.5 mm. The test results below are categorized for drier ground (before the watering) and wetter ground (after the watering).

4.1 Drier Ground

The measured voltages and phase differences for both 100 kHz and 1 MHz operation on drier ground are summarized in Figure 6. Note that these graphs have the appearance of a square wave since the microcontroller alternates the frequencies according to Section 3.1 (indeed it can be seen that for the two different frequencies of operation, the square waves would complement each on the time axis). By inspection of the graphs, the average received signal for 100 kHz operation is approximately 650 mV over the duration of this trial, and the average phase difference between the transmitted and received field is about 80°. For 1 MHz operation, the average received signal is approximately 75 mV over the duration of this trial, and the average phase difference between the transmitted and received field is about 22°.

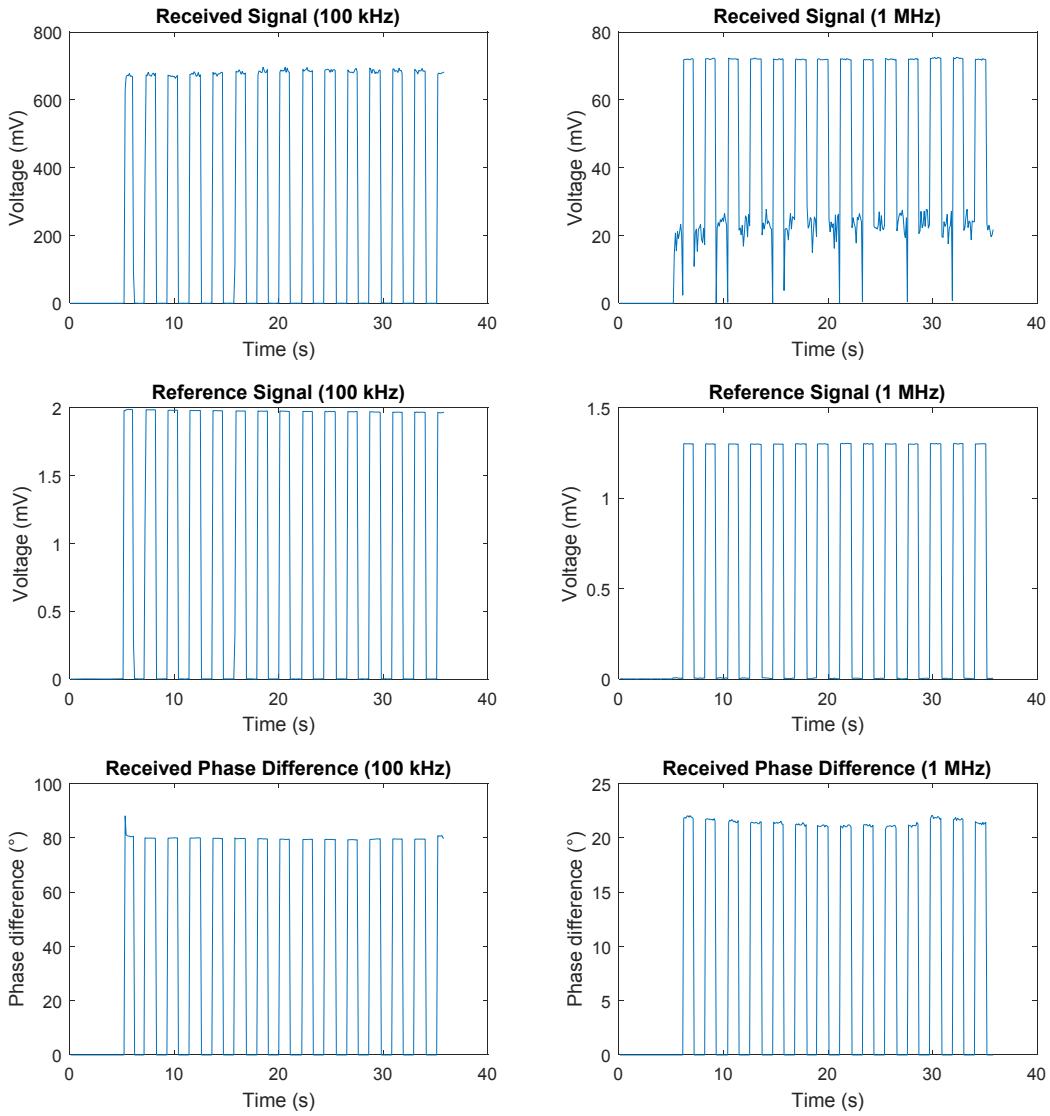

Figure 6. Results for the drier ground test.

4.2 Wetter Ground

The measured voltages and phase differences for both 100 kHz and 1 MHz operation on wetter ground are summarized in Figure 6. Note that these graphs have the appearance of a square wave since the microcontroller alternates the frequencies according to Section 3.1 (indeed it can be seen that for the two different frequencies of operation, the square waves would complement each on the time axis). By inspection of the graphs, the average received signal for 100 kHz operation is approximately 800 mV over the duration of this trial, and the average phase difference between the transmitted and received field is

about 80°. For 1 MHz operation, the average received signal is approximately 85 mV over the duration of this trial, and the average phase difference between the transmitted and received field is about 18°.

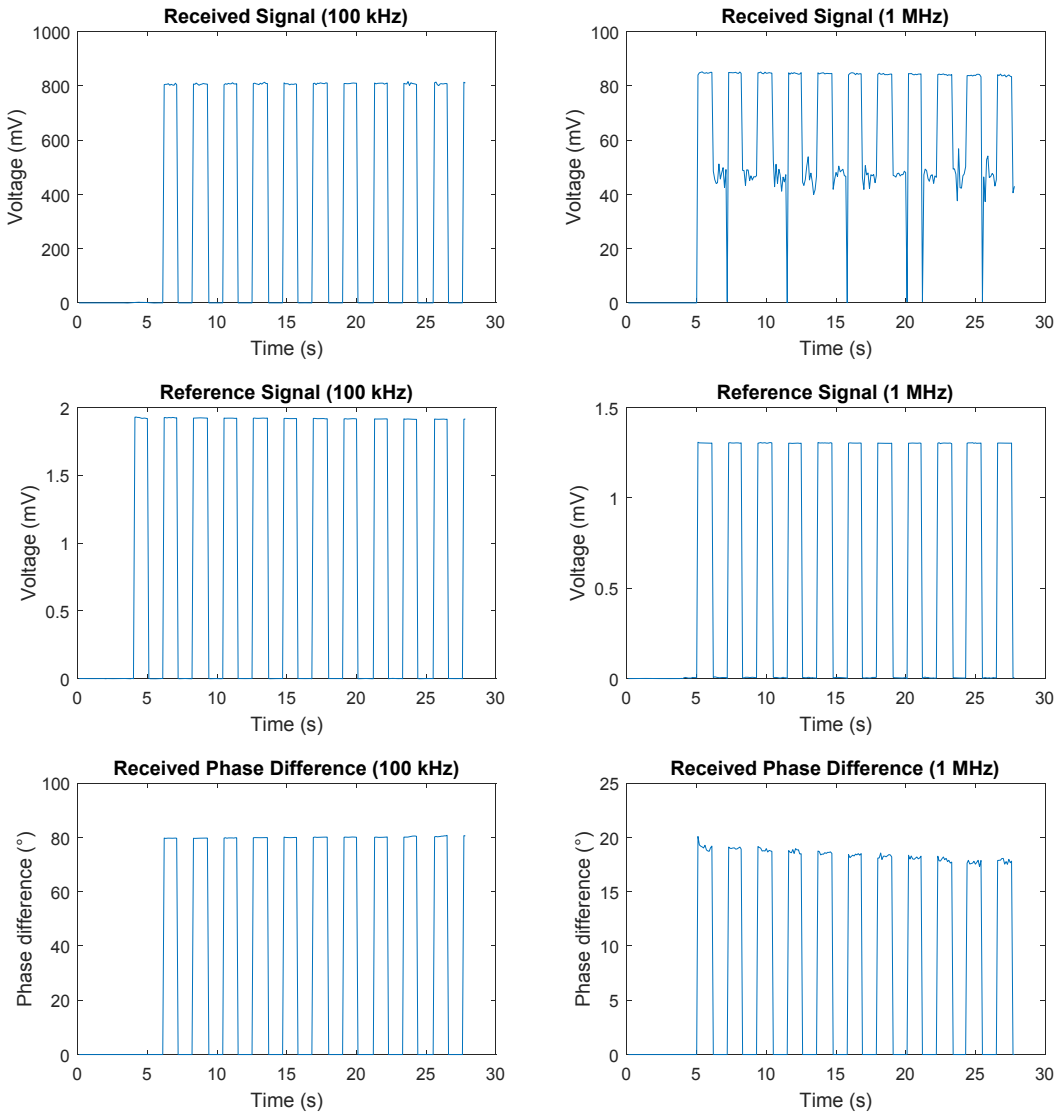

Figure 7. Results for wetter ground test.

It is seen that the recorded values are different for the different ground conditions. Also, the reference signal is approximately 2 mV for 100 kHz operation and 1.3 mV for 1 MHz operation across both soil conditions. Further discussion of these results is presented in section 5.1 after explanation of the calculations.

5 Calculation of Ground Properties

Given the measurements for current on the transmitter, and a voltage on the receiver, it is possible to calculate the impedances at the two different frequencies. From these it is then possible to calculate the relative permittivity and the conductivity of the ground.

Calculation of the ground impedances is straightforward (C-CORE 2017):

$$Z = \frac{V}{I} \tag{1}$$

This should result in calculated impedances for the lower frequency (Z_L) and the higher frequency (Z_H). In addition, there is an impedance calculated from the geometry and the frequency, defined as (C-CORE 2017):

$$Z_0 = \frac{1}{4\pi\varepsilon_0\omega}\left(\frac{1}{r_{11}} + \frac{1}{r_{22}} - \frac{1}{r_{12}} - \frac{1}{r_{21}}\right) \tag{2}$$

where,

ε_0 = permittivity of free space
ω = angular frequency
r_{11} = distance between transmitter probe 1 and receiver probe 1
r_{22} = distance between transmitter probe 2 and receiver probe 2
r_{12} = distance between transmitter probe 1 and receiver probe 2
r_{21} = distance between transmitter probe 2 and receiver probe 1

In the current application, the first two distances are 1 m and the second two are 1.414 m. Hence:

$$Z_0 = \frac{2 - \sqrt{2}}{4\pi\varepsilon_0\omega} \tag{3}$$

The complex permittivity is represented as (C-CORE 2017):

$$\varepsilon_c = \varepsilon + \frac{j\sigma}{\omega\varepsilon_0} \tag{4}$$

And for lower and higher frequencies can be calculated as:

$$\varepsilon_{C,L} = \frac{2Z_0}{Z_L} - 1 = \varepsilon + \frac{j\sigma}{\omega_L\varepsilon_0} \tag{5}$$

$$\varepsilon_{C,H} = \frac{2Z_0}{Z_H} - 1 = \varepsilon + \frac{j\sigma}{\omega_H\varepsilon_0} \tag{6}$$

Taking the magnitudes of the right hand sides of equations (5) and (6) and subtracting them:

$$\varepsilon^2 + \left(\frac{\sigma}{\omega_L \varepsilon_0}\right)^2 - \varepsilon^2 + \left(\frac{\sigma}{\omega_H \varepsilon_0}\right)^2 = \left(\frac{2Z_0}{Z_L} - 1\right)^2 - \left(\frac{2Z_0}{Z_H} - 1\right)^2 \tag{7}$$

For the present application, $\omega_H = 10\omega_L$. Hence equation (7) can solved for conductivity as:

$$\sigma \approx \omega_L \varepsilon_0 \sqrt{\left(\frac{2Z_0}{Z_L} - 1\right)^2 - \left(\frac{2Z_0}{Z_H} - 1\right)^2} \tag{8}$$

Back substitution in the magnitude of (5) and solving for relative permittivity yields:

$$\varepsilon = \sqrt{\left(\frac{2Z_0}{Z_L} - 1\right)^2 - \left(\frac{\sigma}{\omega_L \varepsilon_0}\right)^2} \tag{9}$$

Note that the back substitution could also be applied to equation (6).

5.1 Application of Calculations to Prototype

For the prototype, it is noted that the receiving amplifier has a nominal gain of 100, and the measured reference signal is across a 1 kΩ resistor. That is, a 1V signal represents 1 mA. For convenience, the results from Sections 4.1 and 4.2 are summarized in Table 1, and presented with better precision resulting from averaging the readings over time.

Table 1. Summarized ground properties sensor test results.

Ground Condition	Lower Frequency (100 kHz)			Higher Frequency (1 MHz)		
	Received (mV)	Phase diff. (°)	Reference (mV)	Received (mV)	Phase diff. (°)	Reference (mV)
Drier	671	79.8	1.95	72.0	21.4	1.30
Wetter	808	80.0	1.92	84.4	18.4	1.30

It is noted that the reference signal is much lower than the nominal 0.5 mA to 1 mA operation, by a couple orders of magnitude. One explanation is that the ground contact was not secure enough between probe and the soil, and hence a larger-than-expected impedance was encountered leading to non-compliance of the current source. Regardless, the ground properties were calculated in each case, according to the method outlined in Section 5. These are presented in Table 2.

Table 2. Calculated ground properties.

Ground Condition	Permittivity (relative)	Conductivity (S/m)
Drier	1.98	1.80×10^{-5}
Wetter	1.55	1.42×10^{-5}

The calculated values are low, however within order-of-magnitude agreement with values for ground properties outlined in a ground wave propagation ITU report (International Telecommunications Union 2007). However, the trend is reversed from what would be anticipated. That is, the wetter ground should have higher values for permittivity and conductivity.

One explanation for this builds upon the explanation for the low reference current. Assuming poor ground contact, the transmitter probes are basically acting as a dipole radiating very near the ground. The receiver probes would also be acting as a receiving dipole. In the absence of a significant induced current in the ground, the only received voltage would be owing to a reception of a ground wave from the radiating transmitter dipole. According to the ITU report (International Telecommunications Union 2007) propagation of a ground wave is aided by wetter ground; that is, a received field for a given distance would be higher for wet ground than dry ground. It is entirely possible that a ground properties sensor could be designed and optimized based on this operating principle; however, for the current application, it represents off-nominal behavior and is only an explanation which fits the observed data.

6 Followup Testing

Upon delivery to DRDC Suffield, the prototype exhibited some off-nominal behavior. It was sent back to C-CORE for examination and modifications where necessary. These are identified and explained below.

First, it was noticed that the output from the signal transformer was very noisy. This was traced back to cold solder joints in the assembly. These were fixed; however it was noticed that the output levels for the signal transformer at the lower frequency (100 kHz) were much lower than anticipated. It was decided to remove this transformer as it added an element of uncertainty to the performance of the prototype. The original intention was to have magnetic isolation of the two different power supplies—one each for the transmitter and receiver—thereby eliminating the risk of coupling of the transmitted current through the ground connections. However, upon further experimentation with the design, it was concluded that the received signal was much stronger than any of the observed coupling, and hence the isolation was deemed no longer necessary.

Second, the observed voltage across a test 10 kΩ resistor was both low and dependent upon frequency. It is noted that the output is a current source, and hence a lower load resistor would result in a lower voltage. Also, the observed frequency dependence was a result of oscilloscope loading: use of a high-impedance 10x probe revealed that the outputs at both 100 kHz and 1 MHz were the same.

Finally, it was noted that the output voltage levels at 1 MHz were very low once connected through the bare coaxial RG59 cables. This was traced to the fact that these cables have a distributed capacitance per length; over a length of 1 meter, this capacitance is significant enough to provide a parallel shunt impedance with the intended load, and hence the observed voltage levels dropped. To combat this, it is recommended that the prototype be used with bare wire as the probes. A further iteration of the design could address this.

6.1 Testing with a Resistor Bridge

It is useful to provide a baseline test which is not dependent on soil type so as to ensure proper operation of the prototype. This test was a bridge of resistances which modelled a distributed impedance of the ground, seen in Figure 8.

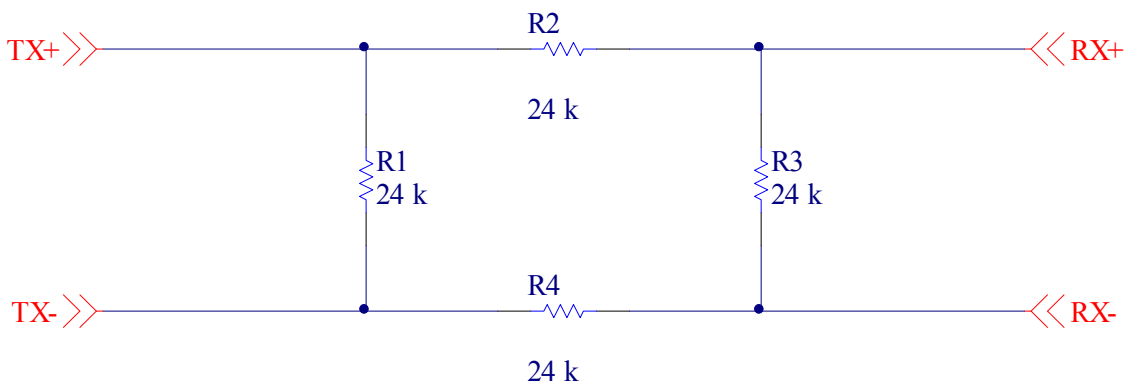

Figure 8. Resistor bridge for testing.

Note that the input impedance of the receiver also factors into the calculation, and manifests itself as a parallel resistance across RX+ and RX-. It can be shown using straightforward circuit analysis that the anticipated voltage across RX+ and RX- is:

$$V_{out} = \frac{RZI_S}{3R + 4Z} \tag{10}$$

Where R is the bridge resistor size (24 kΩ), Z is the input impedance (78 kΩ) of the receiver, and I_s is the current of the source. The results are shown in Figure 9. It was measured that for the 100 kHz signal, the current is 71 µA, and the output voltage was 0.343 V, which gives good agreement according to the formula above. It was measured that for the higher frequency, there was a higher measured voltage for the same current source. This could be explained by the fact that there was a parasitic inductance in the test setup; the leading phase difference lends corroborates this explanation. This would lead to a higher observed voltage. It is deemed that for a proof-of-concept, where order-of-magnitude agreement is sought, this is still satisfactory. This is something that could be addressed in a further iteration of the prototype.

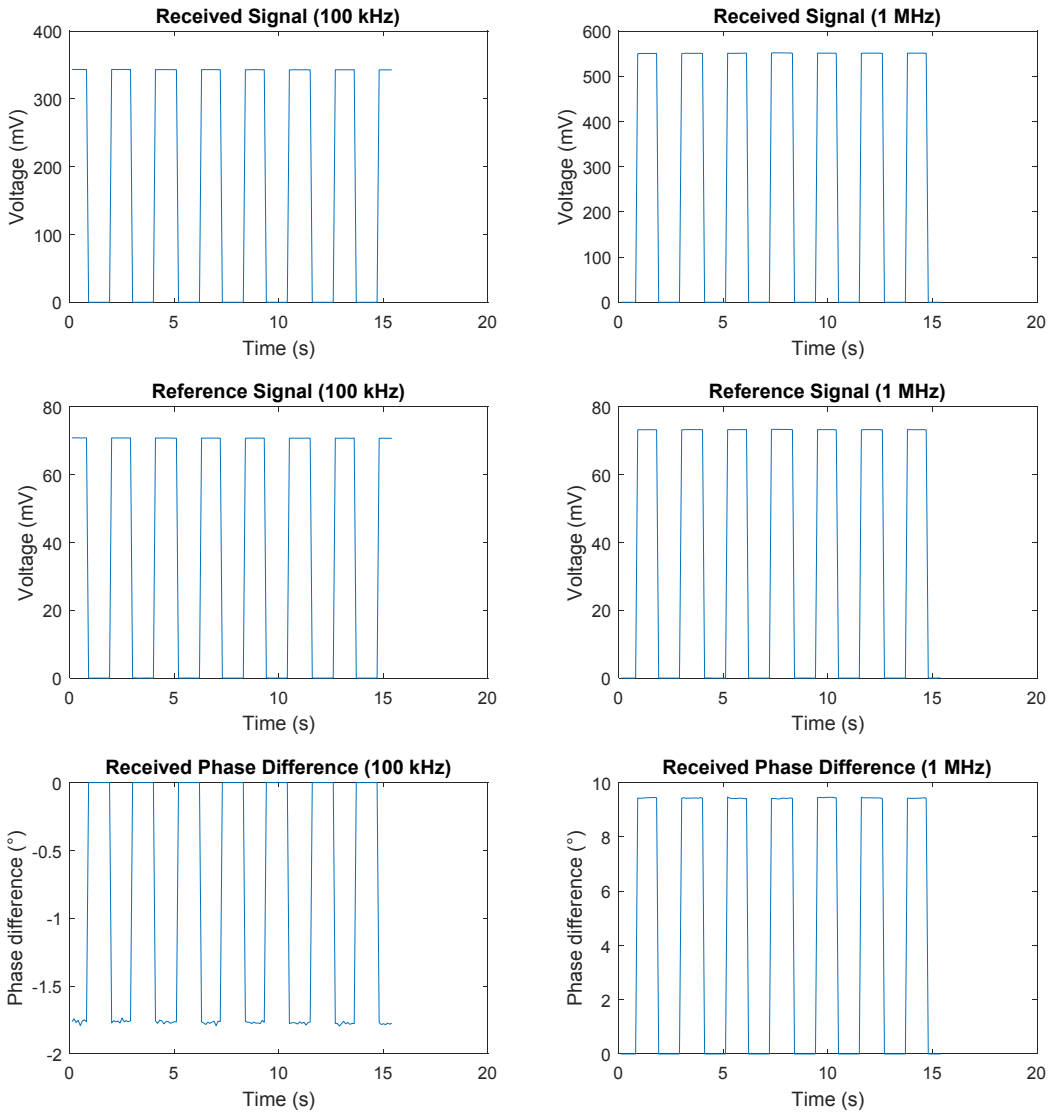

Figure 9. Test results for 24 kΩ resistor bridge.

6.2 Testing in a Bucket of Damp Sand

To test the apparatus, the leads were placed in a 5-gallon bucket of damp sand arranged in a 10cm x 10cm square. The results are shown in Figure 10. The relevant averaged data are summarized in Table 3.

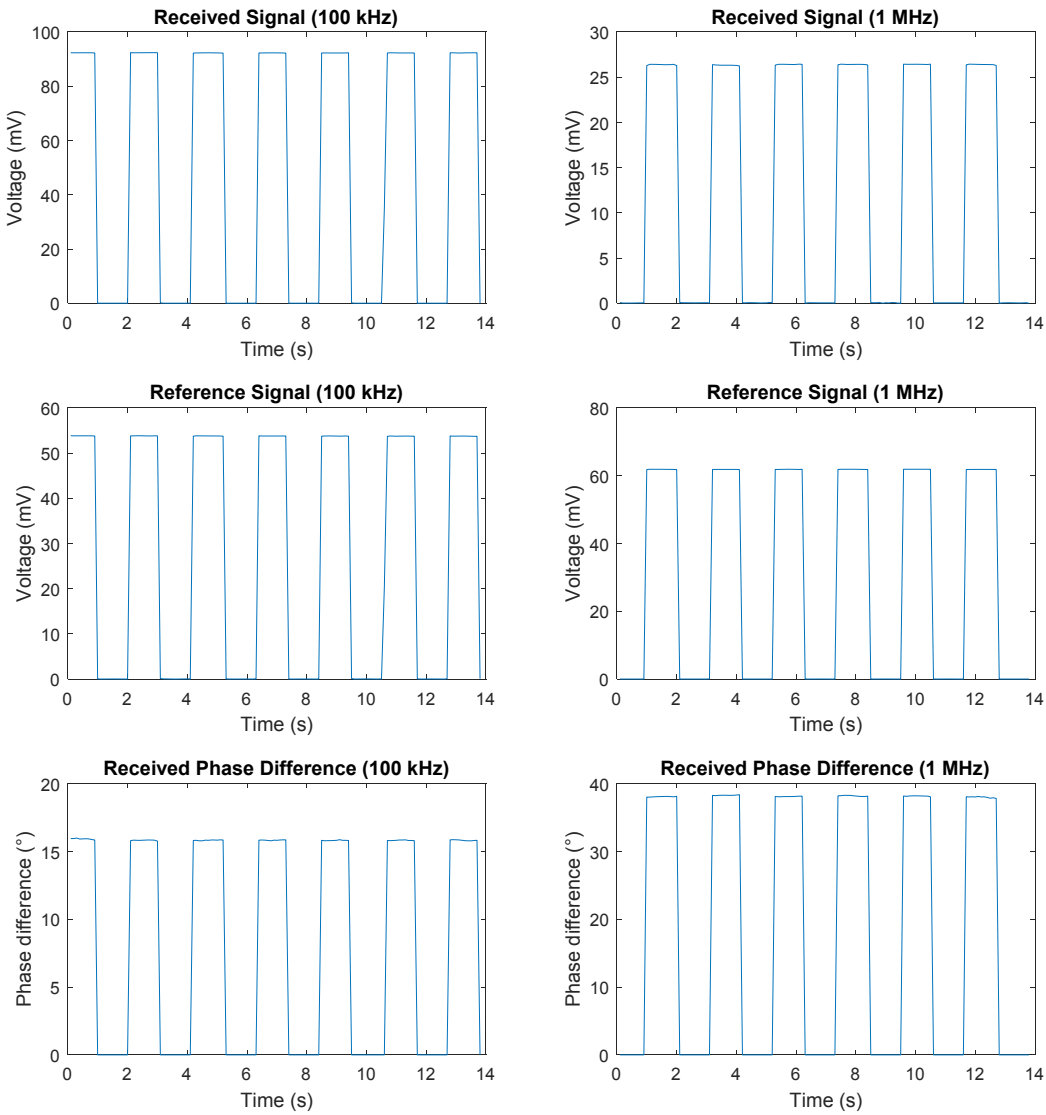

Figure 10. Results for damp sand.

Table 3. Data for damp sand.

Ground Condition	Lower Frequency (100 kHz)			Higher Frequency (1 MHz)		
	Received (mV)	Phase diff. (°)	Reference (mV)	Received (mV)	Phase diff. (°)	Reference (mV)
Damp sand	92.2	15.8	53.8	26.4	38°	61.8

Following the calculation procedure in Section 5, it was found that the magnitude of the permittivity was 37.2 and the conductivity was 5 x 10^{-4} S/m. In addition, a second method of calculation provided by LRDC (elaborated upon in Appendix B) was shown to produce results of, at 100 kHz:

$$\varepsilon = \frac{2Z}{j\omega C_0 |Z|^2} - 1 = 25.6 - j93.9 \tag{11}$$

and

$$\sigma = \frac{2\varepsilon_0 \cos\phi}{C_0 |Z|} = 4.9 \times 10^{-4} \tag{12}$$

And at 1 MHz:

$$\varepsilon = \frac{2Z}{j\omega C_0 |Z|^2} - 1 = 23.2 - j30.9 \tag{13}$$

and

$$\sigma = \frac{2\varepsilon_0 \cos\phi}{C_0 |Z|} = 0.0017 \tag{14}$$

The agreement between the two methods is good for conductivity at the low frequency, and permittivity at the higher frequency. According to the ITU ground propagation report (International Telecommunications Union 2007), these results are very roughly in alignment with their characterization of medium dry ground, which has a relative permittivity of 15 and a conductivity of 0.001.

6.3 Testing in a Bucket of Dry Sand

The same bucket of sand was allowed to dry out, and a series of measurements were taken again. The measurements are presented in Figure 11.

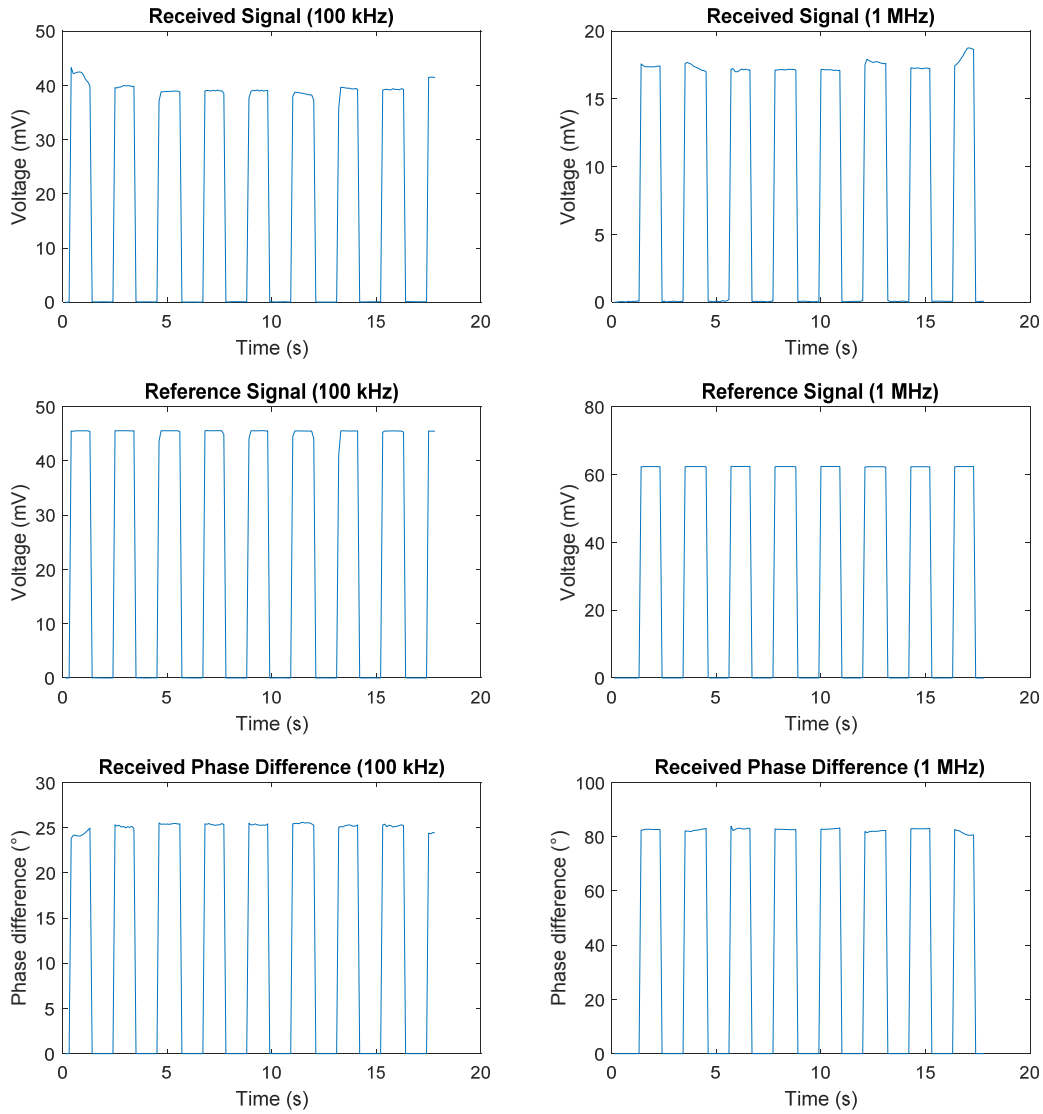

Figure 11. Results for dry sand.

A summary of the results of the calculations using the various methods is shown in Table 4.

Table 4. Calculation results for dry sand.

Calculation Method	Permittivity (relative)	Conductivity (S/m)
Section 5	52.7	0.001
Appendix B – 100 kHz	81 – j175	9.72×10^{-4}
Appendix B – 1 MHz	58.5 – j7.8	4.36×10^{-4}

Once again, the agreement between the two methods is good for conductivity at the low frequency, and permittivity at the higher frequency. Note that, as in Section 5.1, these results appear counterintuitive: the drier sand has a notably higher relative permittivity and conductivity. Still further testing and analysis will be required to explain this discrepancy.

7 Conclusions and Recommendations

A prototype was constructed that was intended to prove the concept of measuring ground properties with the methods outlined in a prior report (C-CORE 2017). The prototype was built with basic commercial off-the-shelf (COTS) components and modules. It was then deployed in the field and was tested for functionality in a realistic environment.

The prototype was found to have discriminated between different soil types, as evidenced by the different readings for drier and wetter ground. However, its behaviour was off-nominal. This had originally been attributed to poor ground contact. Further re-testing revealed that the prototype measured at least order-of-magnitude realistic ground characteristics, but once again showed trends that were contrary to expectation: that is, higher permittivity and conductivity values for drier conditions.

In addition, there are a number of improvements that could be considered for a future iteration of the sensor. These are enumerated below.

- The probes could be designed to have better ground contact. It was found from intermediate testing of the prototype components that contact on top of grass is not as reliable as contact with the soil itself. This could be remedied by replacing the smooth casters with spiked wheels or some other means of ensuring penetration into the soil. In addition, a coil or additional weight could be added to the probe legs to add pressure and ensure ground contact.
- The design of the mechanical frame detailed in the prior report (C-CORE 2017) could be implemented. Due to cost constraints in this contract, it was not possible to fabricate that frame. The design could be updated to include the ground penetrating wheels noted above.
- The power supply noise could be reduced. It was found in unit testing that harmonics corresponding to the power supply switching circuitry were present in the received signal spectrum. These harmonics did not impact the readings for the tests of Section 4 because of the selected frequencies and tight resolution bandwidth. A higher grade power module for generating the bipolar supplies required by the operational amplifier circuitry could be used to ensure that the impacts are minimized.
- A custom PCB could be fabricated for both the transmitter and receiver module as alluded to in Section 3.1. This would allow integration of other designated hardware and also allow a greater degree of interfacing. The PicoScope would not be required as custom ADC circuitry could be used to perform the measurements. The sensor could have on-board storage for the sensor readings which are then retrieved at a later time, eliminating the need for a designated PC. There could also be USB access for managing the settings of the sensor.

In addition, the sensor—either the current manifestation or a future iteration—could be examined for different ground types and conditions. The sensor readings could then be calibrated or otherwise compared against known ground types. Further testing would be required to demonstrate the proof of concept and to explain the apparent counterintuitive measurements the prototype makes. Implementing some or all of these recommendations would result in a more mature design.

8 References

C-CORE. 2013. "Detection of Command Wires - Final Report." Report R-13-005-899 V2. C-CORE.

———. 2014. "Vehicle Mounted Command Wire Detection - Final Report." Report R-13-106-1090 V2. C-CORE.

———. 2017. "Ground Sensor Prototype Design." Report R-16-080-1336. C-CORE.

International Telecommunications Union. 2007. "Ground Wave Propagation Curves Recommendation." ITU-R P.368.9. International Telecommunications Union.

Appendix A: Prototype Schematics

Transmitter

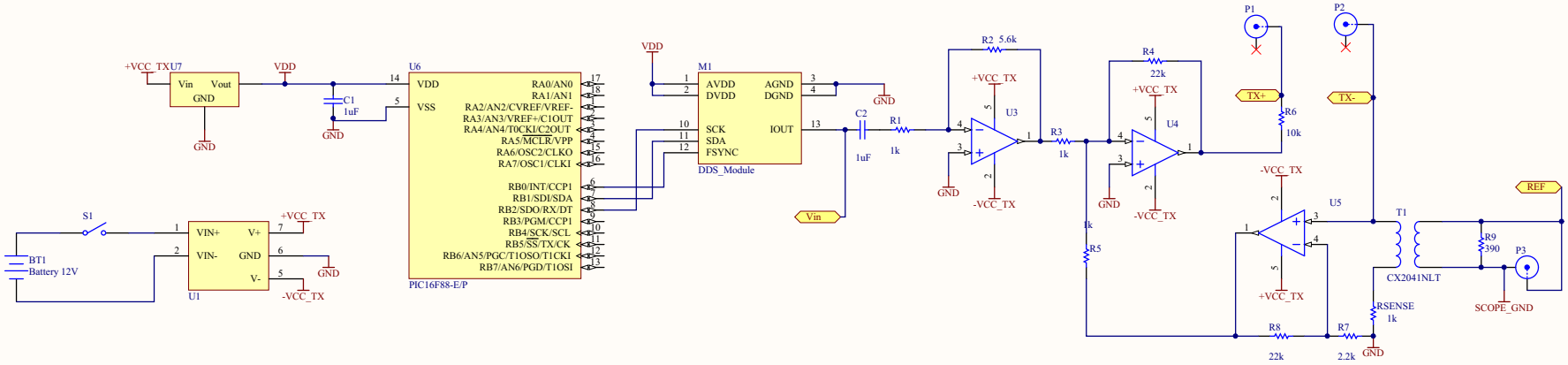

Receiver

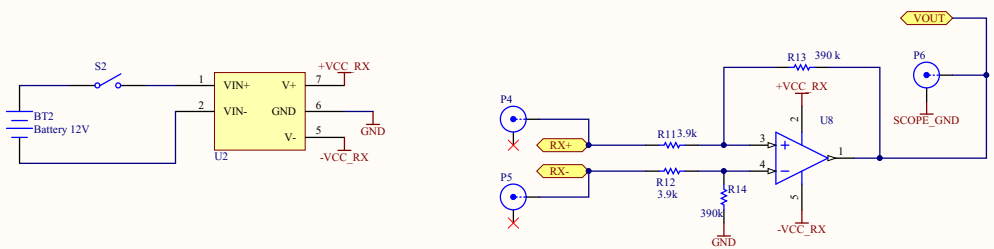

REV.	DESCRIPTION	DATE	BY
1			
2			
3			
4			
5			
6			
7			

		APPROVALS		INITIAL	DATE
CLIENT	Defence Research and Development Canada				
CLIENT DRAWING NO.		DRAWN BY	David Green		
NEXT HIGHER LEVEL OF DRAWING(S):		CHECKED BY			
N/A		APPROVED BY	David Green		
DRAWING FILE NAME	Ground Properties Sensor DEA-1336-1000.SchDoc				

C-core
Captain Robert A. Bartlett Building
Morrissey Road St. John's NL Canada A1B 3X5
T: (709) 737-8354 | F: (709) 737-4706 | www.c-core.ca

TITLE	Ground Properties Sensor
PROJECT	Ground Properties Sensor.PrjPCB
DWG. NO.	DEA-1336-1000
SCALE n/a	SIZE A3 · SHEET 1 OF 1 · REV. 1.0

Appendix B: Theory of Quadrupole Ground Probe Detector

Theory of Quadrupole Ground Probe Detector

This theory applies to a rectangular array of four probes touching the ground. A current is forced through two of them and the voltage is measured between the other two. The frequency is low, so that the process is quasi-static and electrostatic theory is applicable. The ground is conducting with relative permittivity ε and conductivity σ. We assume the conventional time dependence is of the form $e^{j\omega t}$. Then the complex relative permittivity of the ground is given by:

$$\varepsilon = \varepsilon' - j\frac{\sigma}{\omega\varepsilon_0} \tag{1}$$

where ε_0 is the permittivity of free space.

If this planar array were entirely in free space, we could consider a pair of transmitting probes with charges $\pm q$. The potential at a distance r from a single charge is given by:

$$V = \frac{q}{4\pi\varepsilon_0 r} \tag{2}$$

Therefore, the potential difference at the receiving probes would be:

$$V = \frac{q}{4\pi\varepsilon_0}\left(\frac{1}{r_{11}} + \frac{1}{r_{22}} - \frac{1}{r_{12}} - \frac{1}{r_{21}}\right) \tag{3}$$

where the subscripts on r indicate the transmitting and receiving probes. Now current is the rate of change of charge, so that $I = j\omega q$, and this permits us to write the transfer impedance of the array, Z_0, as:

$$Z_0 = \frac{V}{I} = \frac{1}{j4\pi\varepsilon_0\omega}\left(\frac{1}{r_{11}} + \frac{1}{r_{22}} - \frac{1}{r_{12}} - \frac{1}{r_{21}}\right) = \frac{1}{j\omega C_0} \tag{4}$$

Here, we have introduced a variable of the dimensions of capacitance, C_0, which represents the transfer impedance of the probes in free space:

$$C_0 = \frac{4\pi\varepsilon_0}{\left(\frac{1}{r_{11}} + \frac{1}{r_{22}} - \frac{1}{r_{12}} - \frac{1}{r_{21}}\right)} \tag{5}$$

In reality, the probes are located at the interface between air and ground. The modifications to the theory are related to the field from a charge near a dielectric half space. This is described in most elementary texts. When the charge is located within the dielectric, the electric field can be deduced by replacing the charge by an effective charge:

$$q \rightarrow \frac{2q}{\varepsilon + 1} \tag{6}$$

In our case, the charges are on the surface but allowing them to be buried just beneath it makes no difference because transverse fields (parallel to the surface) are continuous across it. As a result, the mutual impedance and the mutual capacitance are modified by the factor $2/(\varepsilon + 1)$. Therefore, we have:

$$Z = \frac{2Z_0}{\varepsilon + 1} \tag{7}$$

This can be rearranged to yield:

$$\varepsilon = \frac{2Z_0}{Z} - 1 = \frac{2}{j\omega C_0 Z} - 1 \tag{8}$$

Denoting real and imaginary parts of Z by single and double primes, respectively, this yields:

$$\varepsilon = \frac{2(Z' - jZ'')}{j\omega C_0 |Z|^2} - 1 \tag{9}$$

From (1) we have:

$$\begin{aligned} \varepsilon' &= \frac{-2Z''}{\omega C_0 |Z|^2} - 1 = \frac{-2\sin\phi}{\omega C_0 |Z|} - 1 \\ \sigma &= \frac{2\varepsilon_0 \cos\phi}{C_0 |Z|} \end{aligned} \tag{10}$$

where ϕ is the phase angle. For capacitances in general, the voltage lags the current, so that the phase angle is negative. For free space, the phase angle is -90 deg. and $|Z| = 1/(\omega C_0)$. Therefore $\varepsilon = 1$ and $\sigma = 0$, as expected.

From (5), when the probe geometry is a square of side 1 m, the transfer capacitance, C_0, in free space is close to 190 pF.

Appendix C: Revised Schematics

Transmitter

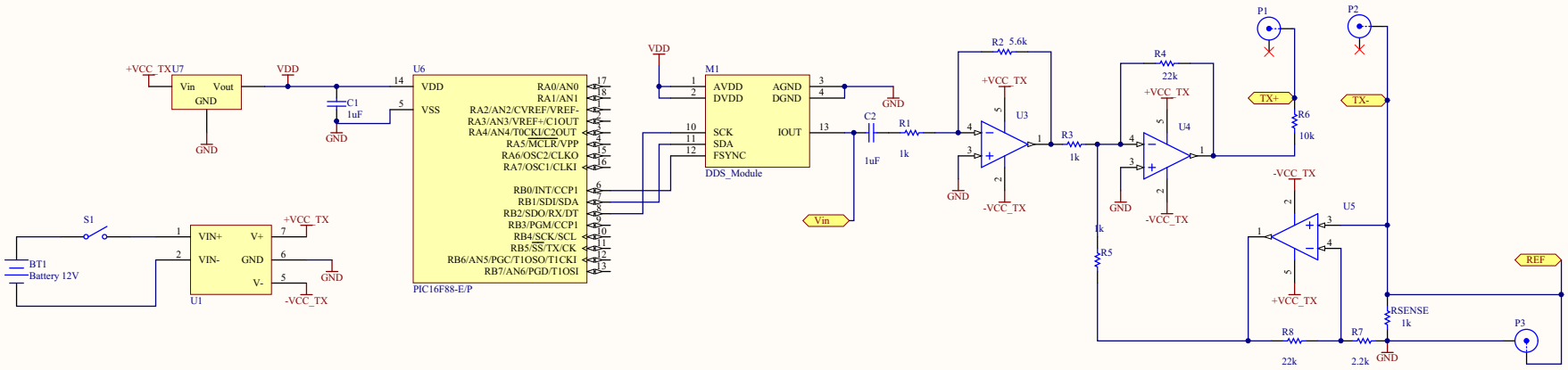

Receiver

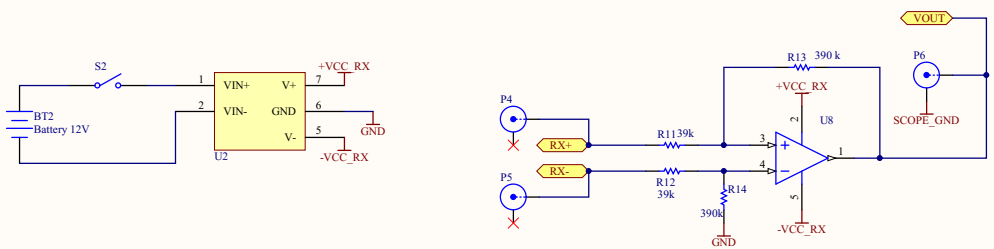

REV.	DESCRIPTION	DATE	BY
1			
2			
3			
4			
5			
6			
7			

		APPROVALS		INITIAL	DATE
CLIENT	Defence Research and Development Canada				
CLIENT DRAWING NO.		DRAWN BY	David Green		
NEXT HIGHER LEVEL OF DRAWING(S):		CHECKED BY			
N/A		APPROVED BY	David Green		
DRAWING FILE NAME	Ground Properties Sensor DEA-1336-1000.SchDoc				

C-core
Captain Robert A. Bartlett Building
Morrissey Road St. John's NL Canada A1B 3X5
T: (709) 737-8354 | F: (709) 737-4706 | www.c-core.ca

TITLE	Ground Properties Sensor
PROJECT	Ground Properties Sensor
DWG. NO.	DEA-1336-1000
SCALE n/a	SIZE A3 · SHEET 1 OF 1 · REV. 1.0

LAST PAGE OF DOCUMENT

DOCUMENT CONTROL DATA

*Security markings for the title, authors, abstract and keywords must be entered when the document is sensitive

1. ORIGINATOR (Name and address of the organization preparing the document. A DRDC Centre sponsoring a contractor's report, or tasking agency, is entered in Section 8.) C-CORE Captain Robert A. Bartlett Building Morrissey Road St. John's, NL Canada A1B 3X5	2a. SECURITY MARKING (Overall security marking of the document including special supplemental markings if applicable.) CAN UNCLASSIFIED 2b. CONTROLLED GOODS NON-CONTROLLED GOODS DMC A

3. TITLE (The document title and sub-title as indicated on the title page.)

Modeling and Experimental Support for Detection of Linear Conductors

Task Authorization 4: Ground Properties Sensor

4. AUTHORS (Last name, followed by initials – ranks, titles, etc., not to be used)

Green, D.; Fowler, C.; Royle, M.

5. DATE OF PUBLICATION (Month and year of publication of document.)	6a. NO. OF PAGES (Total pages, including Annexes, excluding DCD, covering and verso pages.)	6b. NO. OF REFS (Total references cited.)
March 2018	37	4

7. DOCUMENT CATEGORY (e.g., Scientific Report, Contract Report, Scientific Letter.)

Contract Report

8. SPONSORING CENTRE (The name and address of the department project office or laboratory sponsoring the research and development.)

DRDC – Suffield Research Centre
Defence Research and Development Canada
P.O. Box 4000, Station Main
Medicine Hat, Alberta T1A 8K6
Canada

9a. PROJECT OR GRANT NO. (If appropriate, the applicable research and development project or grant number under which the document was written. Please specify whether project or grant.)	9b. CONTRACT NO. (If appropriate, the applicable number under which the document was written.)
02da—Manoeuvre through Adaptive Dispersed Operations (ADO)	W7702-175832
10a. DRDC PUBLICATION NUMBER (The official document number by which the document is identified by the originating activity. This number must be unique to this document.)	**10b. OTHER DOCUMENT NO(s). (Any other numbers which may be assigned this document either by the originator or by the sponsor.)**
DRDC-RDDC-2019-C019	

11a. FUTURE DISTRIBUTION WITHIN CANADA (Approval for further dissemination of the document. Security classification must also be considered.)

Public release

11b. FUTURE DISTRIBUTION OUTSIDE CANADA (Approval for further dissemination of the document. Security classification must also be considered.)

12. KEYWORDS, DESCRIPTORS or IDENTIFIERS (Use semi-colon as a delimiter.)

Electromagnetics; soil moisture; soil parameters; permittivity; conductivity

13. ABSTRACT/RÉSUMÉ (When available in the document, the French version of the abstract must be included here.)

A principal factor in buried conductor detection is consideration of the ground properties. In particular, the conductivity and relative permittivity of the soil can have impacts on the propagation of transmitted waves and reradiated fields, as well as the resonances that can be developed in a length of conductor for schemes that exploit this phenomenon. A sensor prototype was developed to measure both conductivity and relative permittivity. The sensor design is described in detail and test results from a functional test in a simulated environment.